Pressure and Flow Interplay in Aortic Dilation Using 4D Flow Magnetic Resonance Imaging

Kevin Bouaou[1], Thomas Dietenbeck[1], Gilles Soulat[2], Sophia Houriez--Gombaud-Saintonge[1,4], Ioannis Bargiotas[1], Alain De Cesare[1], Umit Gencer[2], Alain Giron[1], Alban Redheuil[1], Emilie Bollache[1], Didier Lucor[3], Elie Mousseaux[2], Nadjia Kachenoura[1]

[1]Sorbonne Université, INSERM, CNRS, Laboratoire d'Imagerie Biomédicale, Paris, France
[2]Hôpital Européen Georges Pompidou, Paris, France
[3]LIMSI, CNRS, Université Paris-Saclay, Orsay, France
[4]ESME Research LAB, Paris, France

Abstract

Ascending thoracic aortic aneurysms (ATAA) are defined by a silent dilation of the ascending aorta (AA). Although maximal aortic diameter is currently used for surgery planning, a high proportion of patients with low diameters ending up with aortic dissection. Our purpose was to propose a fine and comprehensive quantitative evaluation of pressure-flow-wall interplay from 4D flow MRI data in the setting of aortic dilation.

We studied 12 patients with ATAA (67±14 years, 7 male) and 12 healthy subjects (63±12 years, 8 male) who underwent 4D flow MRI acquisition. The segmented velocity fields were used to estimate: 1) local AA pressure changes from Navier-Stokes-derived relative pressure maps (AADP), 2) AA wall shear stress (AAWSS) by estimating local velocity derivatives at the aortic borders, 3) aortic flow vorticity using the λ_2 method (AAV).

AADP was significantly and positively associated with both AAV ($r=0.55$, $p=0.006$) and AAWSS ($r=0.69$ $p<0.001$). Such associations remained significant after adjustment for maximal diameter, age and BSA.

Local variations in pressures within the aorta, rendered possible while using 4D flow MRI, are associated with flow disorganization as quantified by vorticity and with the increase in the stress exerted on the aortic wall, as quantified by wall shear stress.

1. Introduction

Ascending thoracic aortic aneurysm (ATAA) is an asymptomatic dilatation of the ascending aorta that can ultimately lead to aortic dissection and a subsequent increase in morbi-mortality. Although such dilatation can be observed in specific diseases such as Marfan, Turner Syndrome or Ehlers-Danlos, it can also be present in the general population [1]. Clinical guidelines for the assessment of aneurysm are mostly based on maximal diameters to evaluate the risk of rupture or dissection and intervention planning [2]. However, the understanding and the prediction of ATAA progression are not well established yet and aortic dissection is frequently occurring on normally sized or mildly dilated aortas.

The added value of 4D flow (time-resolved 3D velocity-encoded) MRI for the visualization and characterization of aortic systolic flow disorganization was shown in several studies and in various aortic root and valve disease conditions [3]. Such abnormal flow patterns were characterized using different quantitative parameters [4], including: 1) wall shear stress (WSS), which is the frictional force exerted by blood flow on the aortic wall [5], 2) flow eccentricity, which measures systolic peak flow displacement from the aortic centerline [4], 3) vortical flow, which is associated to the blood flow rotation around a specific axis [6]. Such indices are intimately associated to local aortic pressures since blood flow circulation patterns are driven by local pressure gradients.

Despite well-established theoretical associations between pressure gradients and blood flow patterns and their changes with disease, there are no studies in the literature focusing on simultaneous evaluation of pressure gradients and indices quantifying flow disorganization using MRI. Thus, our aims were to: 1) non-invasively estimate local aortic pressure gradients by combining Navier-Stokes equations and 4D flow MRI velocity fields [7] in parallel to aortic flow vorticity and WSS, 2) to evaluate local associations between pressure gradients and flow-derived quantitative indices in a group of patients with a dilated aortic root and a tricuspid aortic valve, paired for age with healthy subjects.

2. Material and Methods

2.1. Population and data acquisition

4D flow MRI data were acquired in 24 subjects including 12 patients with a ATAA (67±14 years, 7 males) and 12 age-matched healthy subjects (63±12 years, 8 males).

MRI was performed on a 3T imaging system (Mr750w GEM, GE Healthcare, Milwaukee, WI, USA) with a 32-channel cardiac phased-array coil. 4D flow data were acquired during free-breathing with ECG gating in a sagittal oblique volume encompassing the thoracic aorta, using the following scan parameters: echo time=1.7 ms, repetition time TR=4.3-4.4 ms, flip angle=15°, spatial resolution=1×1.48×2.38 mm^3, and velocity encoding=250 cm/s in all directions. Data were reconstructed into 50 temporal phases.

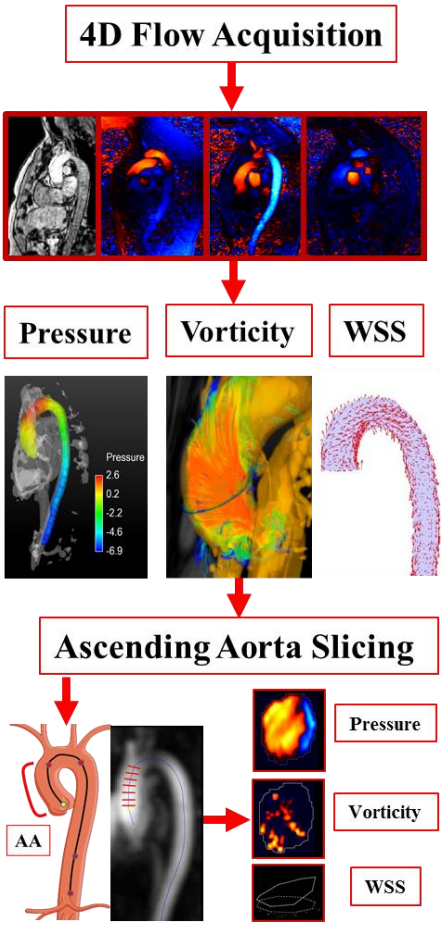

Figure 1: 4D flow MRI data processing pipeline.

2.2. MRI 4D flow data preprocessing

Phase offset and phase wrapping were corrected according to the 4D flow MRI guidelines [3]. A time-averaged phase-contrast MR angiography (PC-MRA) was then derived from the 3 directional velocities weighted by modulus images, when considering 5 time phases around peak systole, defined as the temporal phase with maximal velocity in the ascending aorta (AA). Such PC-MRA was used to segment the thoracic aortic volume with an explicit active contours algorithm [8] and thus to isolate aortic velocity fields and to define aortic centreline. For each subject, aortic segmentation was used to define 36 cross-sectional planes perpendicular to the centreline from the sino-tubular junction, until the celiac artery bifurcation (Figure 1). The AA segment was then delimited by the sino-tubular junction and the brachiocephalic bifurcation. Finally, maximal diameter perpendicular to the centreline was estimated (AAD_{max}). Algorithms and user interface were written in Matlab 2016 (The Mathworks, Natick, MA).

2.3. Pressure map estimation

First, the pressure gradient (∇P) is estimated using Navier-Stokes equations:

$$\nabla P = -\rho\left(\frac{\partial V}{\partial t} + V.\nabla V\right) + \mu\nabla^2 V + \rho g$$

where ρ is the fluid density (ρ_{blood}=1060 $kg.m^{-3}$), V is the velocity μ is the dynamic viscosity (μ_{blood}=0.0035 $kg.m^{-1}.s^{-1}$) and g is the gravitational force. An initial pressure map P_i is estimated by propagating ∇P from a zero reference point set at the aortic sino-tubular junction. Afterwards the final relative pressure P_f is calculated while verifying that the gradient of P_f is as close as possible to the Navier-Stokes pressure gradient ∇P. This is done through solving the following iterative equation [7]:

$$P_f^{k+1} = (1-\alpha)P_f^k + \frac{1}{6}\alpha\sum_{j=1}^{6}(P_j^k + \nabla P_j.\Delta r_j)$$

where $P_f{}^k$ is the pressure value at the k^{th} iteration, P_j and ∇P_j were relative pressure and pressure gradient of the six orthogonal neighbors, Δr_j is the voxel size and α is a scalar set to 0.5 [7]. Finally, 3D+t aortic pressure maps relative to the zero reference in the valve were obtained.

Such pressure maps were used to calculate in-slice maximal to minimal pressure difference for each time phase. Then its peak during the systolic period is averaged over all AA segment slices (AADP, mmHg).

2.4. Wall shear stress estimation

WSS vectors τ were evaluated on the aortic wall segmentation voxels using the following equation:

$$\vec{\tau} = 2\nu(\varepsilon \cdot \vec{n})$$

where ε represents the deformation rate tensor, $\vec{n}$ the inward normal vector and ν the blood viscosity ($\nu = 3.2e^{-3}$ Pa). The deformation rate tensor is calculated from the local spatial derivatives of the velocity vectors while applying a b-spline interpolation to smooth and reduce the effect of noise at the aortic borders [9]. Finally, WSS at peak systole was averaged on the AA wall (AAWSS, Pa).

2.5. Vortex identification using λ_2-method

The method used for the estimation and quantification of vortex was the λ2-method, which is based on the decomposition of the velocity fields-derived 3x3 Jacobian matrix in a symmetric (S) and antisymmetric (Ω) components corresponding to the shear and the rotational components of the velocity fields, respectively. Considering the Navier Stokes equation, it can be shown that the matrix ($S^2+\Omega^2$) characteristics are related to a local pressure minimum that entails a vortex. A vortex is then defined as the region where two eigenvalues of the ($S^2+\Omega^2$) matrix are negative [10]. Considering that the matrix is real and symmetric, the three eigenvalues λ_1, λ_2, λ_3 of ($S^2+\Omega^2$) are real and can be ordered as $\lambda_1 \leq \lambda_2 \leq \lambda_3$. Thus, a vortex is defined as voxels where $\lambda_2 \leq 0$. Finally, in-slice vorticity peak over the cardiac cycle was averaged through the AA segment (AAV, s^{-1}).

3. Results

Baseline characteristics along with aortic geometrical and hemodynamic measurements within the AA are summarized in Table 1.

Table 1. Subjects characteristics, and ascending aorta MRI measurements. BMI: body mass index. BSA: body surface area. AA: ascending aortic segment, AAD_{max}: maximal AA diameter, AAWSS: AA wall shear stress, AAV: AA vorticity, AADP: AA local difference in pressure.

	Healthy subjects (n=12)	AATA (n=12)
Age (years)	63±12	67±14
Sex (men/women)	7/5	8/4
BMI (kg/m^2)	24.5±3.0	27.5±5.2
BSA (m^2)	1.78±0.23	1.86±0.24
AAD_{max} (mm)	30.0 ± 2.8	40.0 ± 4.1*
AAWSS (Pa)	0.62±0.12	0.53±0.09*
AAV (s^{-1})	66.33±43.38	84.08±56.12
AADP (mmHg)	1.54±0.80	1.21±0.59

*: statistical difference ($p<0.05$) vs. healthy subjects

Figure 2 illustrates in healthy subjects the local pressure homogenization according to aortic geometric remodelling (dilation), throughout the normal process of aging. This result highlights the reliability of our pressure index since it is well known that the pressure equalizes along the arterial tree in normal aging.
The association shown in Figure 2 was not found in the ATAA patients. This might be due to the statistical power, which is even more challenging due to the heterogeneity of our ATTA population. Indeed, patients with the most dilated aorta, as indicated by AAD_{max}/BSA, are not necessarily the most severe.

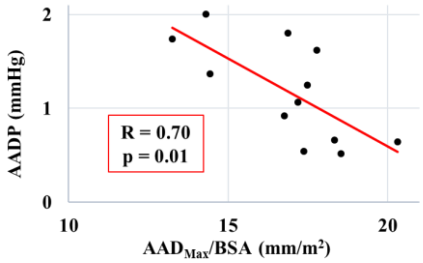

Figure 2: linear association between ascending aorta (AA) local pressure difference index (AADP) and maximal AA diameter indexed to BSA in the group of healthy subjects.

Figure 3 illustrates the associations of local pressure variation index in the AA with both vorticity and wall shear stress. Such positive associations indicate that local pressure variations affect local blood flow, generating blood flow from high to low pressures and subsequently vortices. Such vortices exert an increased shear stress on the surrounding aortic wall. Both associations with AAWSS and AAV remained significant after adjustment for maximal diameter, age and BSA ($p = 0.007$ and $p=0.003$ respectively).

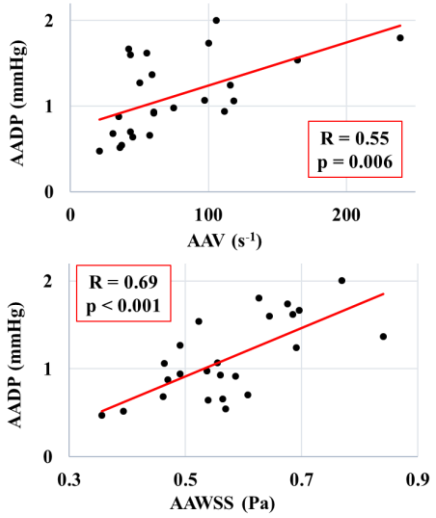

Figure 3: linear associations between ascending aorta (AA) local pressure difference index (AADP) and AA vorticity (AAV) (top) as well as AA WSS (AAWSS) (bottom) on the entire study group.

4. Discussion

In this work, a non-invasive and comprehensive characterization of aortic flow and hemodynamics from 4D flow MRI was provided in the ascending aorta of aneurysmal patients with dilated aortic root and tricuspid aortic valve, matched for age to healthy individuals. To

the best of our knowledge, this is the first study evaluating fine and local variations in pressures within the aorta and illustrating the association between such pressure changes and the underlying flow disorganisation and increase in the stress exerted on the aortic wall.
Previous studies demonstrated the ability of 4D flow MRI acquisitions to estimate separately relative pressures, wall shear stress and vorticity in the thoracic aorta [3]. Values of WSS and vorticity obtained in our population are in the same range than those previously reported [6, 9]. Ascending aorta wall shear stress was extensively used in the setting of bicuspid aortic valve demonstrating its association with histological tissue degradation. An attempt to quantify vorticity within the thoracic aorta has been also reported recently on a small group of patients and simulated data using $\lambda 2$-method [6].
In a recent study, we demonstrated the ability of 4D flow MRI-derived pressure maps and volumetric propagation indices to characterize age-related subclinical changes in thoracic aorta hemodynamics, in association with left ventricular remodelling in a group of 47 subjects aged from 20 to 80 years. The method described in this previous work was applied here to aneurysmal patients and age-matched healthy controls and a fine characterization of local pressure changes was proposed to enhance the understanding of vortex appearance and wall shear stress increase in the setting of pathological aortic dilation. Finally, relative pressure has been shown to be related with age and left ventricular geometry in previous study [7].

The main limitation of our study is the moderate group size. Although the targeted associations were significant despite such small effectives, including more subjects is necessary in order to strengthen conclusions of this preliminary work. In addition, future patient longitudinal follow-up studies are mandatory using all these innovative 4D flow MRI quantitative indices to evaluate their added value, as compared to geometrical characterisation of the aorta.

5. Conclusion

A non-invasive and comprehensive characterization of aortic flow and hemodynamics in the ascending aorta is now provided by 4D flow MRI. Moreover, the derived local variations in pressures within the aorta are associated with flow disorganization as quantified by vorticity and the increase in the stress exerted on the aortic wall, as quantified by wall shear stress.

Acknowledgement

We would like to acknowledge the FRM project ING20150532487 for funding a large part of the technical aspects of this study.

References

[1] Ince H, Nienaber CA. Etiology, pathogenesis and management of thoracic aortic aneurysm. *Nat Clin Pract Cardiovasc Med* 2007; 4: 418–427.

[2] 2014 ESC Guidelines on the diagnosis and treatment of aortic diseases: document covering acute and chronic aortic diseases of the thoracic and abdominal aorta of the adult. *Eur Heart J* 2014; 35: 2873–2926.

[3] Dyverfeldt P, Bissell M, Barker AJ, et al. 4D flow cardiovascular magnetic resonance consensus statement. *J Cardiovasc Magn Reson* 2015; 17: 72.

[4] Burris NS, Hope MD. 4D Flow MRI Applications for aortic disease. *Magn Reson Imaging Clin N Am* 2015; 23: 15–23.

[5] Kauhanen SP, Hedman M, Kariniemi E, et al. Aortic dilatation associates with flow displacement and increased circumferential wall shear stress in patients without aortic stenosis: a prospective clinical study: 4D flow MRI of aortic dilatation. *J Magn Reson Imaging*. Epub ahead of print 18 January 2019. DOI: 10.1002/jmri.26655.

[6] von Spiczak J, Crelier G, Giese D, et al. Quantitative analysis of vortical blood flow in the thoracic aorta using 4D Phase Contrast MRI. *PLOS ONE* 2015; 10: e0139025.

[7] Bouaou K, Bargiotas I, Dietenbeck T, et al. Analysis of aortic pressure fields from 4D flow MRI in healthy volunteers: associations with age and left ventricular remodeling: 4D Flow MRI aortic pressure in Aging. *J Magn Reson Imaging*. Epub ahead of print 4 February 2019. DOI: 10.1002/jmri.26673.

[8] Dietenbeck T, Craiem D, Rosenbaum D, et al. 3D aortic morphology and stiffness in MRI using semi-automated cylindrical active surface provides optimized description of the vascular effects of aging and hypertension. *Comput Biol Med* 2018; 103: 101–108.

[9] Potters WV, van Ooij P, Marquering H, et al. Volumetric arterial wall shear stress calculation based on cine phase contrast MRI: volumetric wall shear stress calculation. *J Magn Reson Imaging* 2015; 41: 505–516.

[10] Haller G. An objective definition of a vortex. *J Fluid Mech* 2005; 525: 1–26.

Bouaou Kevin ; kevin.bouaou@gmail.com
Address for correspondence: Sorbonne Université 15 rue de l'Ecole de Médecine, 75006 PARIS (FRANCE)